2018 7th IEEE International Conference on Biomedical
Robotics and Biomechatronics (Biorob)
Enschede, The Netherlands, August 26-29, 2018

An Active Impedance Controller to Assist Gait in People with Neuromuscular Diseases: Implementation to the Hip Joint of the AUTONOMYO Exoskeleton

A. Ortlieb, R. Baud, T. Tracchia, B. Denkinger, Q. Herzig, H. Bleuler, *Member, IEEE,* and M. Bouri, *Senior Member, IEEE*

***Abstract*—Medical and personal exoskeletons of the lower limbs have successfully been oriented toward persons with complete spinal cord injury (SCI). Persons with less disabling disorders such as muscular dystrophy, multiple sclerosis, hemiplegia or incomplete paraplegia, however require more freedom of motion and greater possibilities for interaction with the device. An assistive strategy relying on a finite-state controller is addressed in the current paper and implemented about the hip flexion-extension during walking. The paper focuses on three major issues. The first one looks at the feasibility and effectiveness of using an active impedance controller with a non-elastic actuator, where typically a transmission ratio of approximately 1:200 allows a torque of about 40 Nm. Secondly, the detection of intention based on volitional motion recognition is evaluated regarding the limitations encountered by the targeted populations. Finally the appropriateness of the three states variable impedance controller is addressed with two pilots, one healthy and one with muscle weakness due to a limb girdle muscular dystrophy (LGMD). The AUTONOMYO exoskeleton used is a lower limb device consisting of three actuated degrees of freedom per leg about the hip (flexion and abduction) and the knee (flexion) while the ankle is semi-rigidly constrained. Results show that the implementation of impedance behaviors on a rigid transmission shows satisfactory performances while it necessitates some active compensation. The controller has been successfully and safely used by both pilots, demonstrating a promising usability to assist people with incomplete gait impairments.**

I. Introduction

Advanced human-robot interaction has been an important field of research for the past decades already. Due to the growing number of robots and applications, the interest in collaborative strategies between man and programmed machines involving physical contact has never been as important as today. In the current paper, we are investigating a collaborative strategy to assist people with gait impairments such as neuromuscular disorders or neurological conditions to walk. Impedance control has been widely used with different approaches and various actuation-transmission units with both upper and lower limbs. Impedance can be used as a soft trajectory corrector where a force is provided by the exoskeleton to attract the end-effector along a defined path such as described in [1] and [2]. Such controllers are trajectory and time dependent and thus quite constraining for the user [3]. Another type of impedance based controller is called triggered assistance and has been mostly implemented with the upper limbs [3]. The architecture of control proposed in the current paper has been largely investigated in the domain of prosthetics for the lower limb (transfemoral and transtibial prosthesis) and is referred to as "finite-state controller". Such controllers are defined by a periodic sequence of states with state-constant impedance that typically simulates a spring and damper behavior [4]–[9]. The transition from one state to another is usually based on different events such as heel strike or toe off which are sensed through force sensors located in the prosthesis. Other events such as a muscle activity or joint angle or velocity are also frequently used [4]–[11]. Several activities such as level walking, stairs or slope ascending / descending and sit-to-stand transition have been studied in these papers. A few studies using foot orthosis [12],[13] or complete lower limb exoskeletons (three using the Indego device [14]–[16] and two with the Hybrid Assistive Limb (HAL) device [17], [18]) implemented similar "finite state" controllers. However, most of these strategies are constructed primarily on events based on the ground reaction forces (e.g. detection of heel strike, displacement of the center of pressure) and also on events related to the motion of the joints.

Figure 1. The AUTONOMYO lower limb exoskeleton with its six actuated degrees of freedom at the hip and knee flexion/extension and at the hip adduction/abduction. On left, a front-side view at 45°. On right, a back-side view at 45°.

*Research supported by ASRIMM (Association Suisse Romande Intervenant contre les Maladies neuro-Musculaires), FSRMM (Fondation Suisse de Recherche pour les Maladies Musculaires) and the Swiss Multiple Sclerosis Society.

All authors are with the Laboratory of Robotic Systems from the Swiss Federal Institute of Technology Lausanne (EPFL), Station 9, 1015 Lausanne, Switzerland (corresponding authors: +41.21.693.7735 – +41.21.693.7346; e-mail: amalric.ortlieb@epfl.ch – mohamed.bouri@epfl.ch).

In the current paper, an active variable impedance controller using a finite-state approach designed for people with residual ability to ambulate is addressed. In order to involve the user in the ambulation process, a strategy requiring motion from the wearer is demanded in order to initiate the stepping. This paper covers different aspects. First, the adequacy of the rigid actuation-transmission unit in the scope of impedance control is examined. Secondly, the control scheme is described and its triggering properties are evaluated. Finally, the controller's impedance is tuned for two pilots, one healthy and one with neuromuscular disease. Gait kinematics and dynamics are collected in order to evaluate the collaboration of the controller and the pilots. The exoskeleton AUTONOMYO (Fig.1) is taken as the investigation platform. The device has been designed to assist people with neuromuscular or neurological impairments where a tradeoff between low impedance of the actuation (high backdrivability) and high power is key. AUTONOMYO counts three actuated degrees of freedom (DoFs) per leg, i.e. two at the hip and knee flexion/extension plus one at the hip adduction/abduction. Actuators, electronics and batteries are remotely located in the back of the user in order to optimize compactness and inertia along the limbs. More details can be found in [19], [20].

II. Identification of the Exoskeleton Hip Joint Actuation Model

A. The transmission and set-up

The current torque model focuses on the hip flexion/extension actuation that is realized by:

- A brushless motor (EC-i 40, Maxon Motor AG, Switzerland)
- A custom three stages gearbox (GP42 HP, Maxon Motor AG, Switzerland) with a 74:1 transmission ratio
- A wire-cable of diameter 2.0 mm (Carlstahl Technocables, Germany) and pulleys with a 3:1 transmission ratio

In order to measure the force transmitted to the exoskeleton's joint, a force sensor (Strain Gauge – Micro Load Cell CZL635, Phidgets Inc, Canada) with a range of 500N is used. The sensor is fastened to the segment in parallel with the femur, at a distance of 0.36m from the exoskeleton's hip joint. It is sampled at 1 kHz and filtered with a low pass filter with a cutoff frequency of 16 Hz. The motor is controlled in current using a custom drive [21] and the position is measured using encoders at the motor level with a resolution of 1000 pulses.

B. Method

In order to model the relationship between the torque at the hip joint and the input current in the motor, a parametric model with linear regression based on least square error minimization is computed for the identification, see (1)-(5). An iterative approach allows augmenting the model while evaluating the relevance of the added term step by step. The expected and candidate variables are: the motor current (motor torque), the torque at joint (efficiency of the transmission), the acceleration (inertia of the actuation), the sinus of the angular joint position (gravitational effect), the velocity (viscous friction, and direction of velocity at low velocities for the dry friction), and the sign of the motor power.

$$Y = X\beta + \varepsilon \tag{1}$$

$$Y = [\tau_{joint}(1), \tau_{joint}(2), \dots \tau_{joint}(n)]^T \tag{2}$$

$$\beta = [\beta_0, \beta_1, \dots \beta_m]^T \tag{3}$$

$$X = \begin{bmatrix} x_1(1) & x_2(1) & \cdots & x_m(1) \\ x_1(2) & & \ddots & \vdots \\ \vdots & & & \\ x_1(n) & & \cdots & x_m(n) \end{bmatrix} \tag{4}$$

$$\min(\epsilon): \quad \hat{\beta} = (X^T X)^{-1} X^T Y \tag{5}$$

Where Y is the external torque applied at the joint (τ_{joint}) vector at different time, X is the matrix of variables or functions of variables that are recorded (variables of the model(s) as presented above such as, joint angular position, velocity, acceleration, torque at joint, power in the motor) at corresponding time, β is the vector of coefficients, ε is the vector of errors and the symbol '^' refers to an estimation of the value.

Data were collected in two manners. First, in position control where the experimenter applies perturbation forces while the motor follows sinusoidal trajectories. Second, a constant current is set to the motor while the experimenter pulls and pushes the segment to induce back and forth motions.

C. Results

Two models are described and evaluated. The first model (6) considers the transmission ratio and a constant efficiency coefficient to express the torque at the hip joint in function of the motor torque. Model 1, i.e. (6), is used as a basic model of reference, it represents the active torque. The second model (7) is the result of the iterative process described previously with equations (1)-(5).

$$\tau_{joint\_1} = \eta_+ \cdot i \cdot \tau_{motor} \tag{6}$$

$$\tau_{joint\_2} = -lmg \cdot \sin(\alpha) - I \cdot \ddot{\alpha} + \eta_{\pm} \cdot i \cdot \tau_{motor} \tag{7}$$

$$lmg = 11.5\ [Nm]$$

$$I = 0.025\ [Kg \cdot m^2/deg]$$

$$\eta_{\pm} = \begin{cases} \eta_+ = 0.55, if\ Power = (\tau_{motor} \cdot \dot{\alpha}) \geq 0 \\ \eta_- = 1.3, if\ Power = (\tau_{motor} \cdot \dot{\alpha}) < 0 \end{cases}$$

Where τ_{joint} is the output torque at the joint measured by the force sensor, τ_{motor} is the input torque at the motor, i is the transmission ratio, α is the angular position at the joint and '$\dot{}$' and '$\ddot{}$' denotes the first and second derivatives over time (joint velocity and acceleration respectively). lmg, I and η are coefficients of the gravitational term, inertial term and torque ratio (efficiency of the transmission) respectively.

Two terms for the efficiency of the transmission, η_+ and η_- are found and are related to the sign of the power. Indeed, when the motor contribution is more important than the opposite forces at the joint (i.e. the power as given by (7) is positive) then losses in the transmission reduce the

transmitted torque from the motor. In this case a factor of 0.55 is found between the torques at joint and at motor. Conversely, when the torque at the joint is bigger than the motor contribution, the power at the motor is negative (i.e. the rotation of the motor is opposed to the torque direction). In this case, the torques at the joint perceived by the motor are diminished due to losses in the transmission. It results that a ratio of 1.3 is obtained between the two torques.

The performances of the fit are difficult to address in a thorough manner. Identification gives more repetitive results with a constant motor torque target while the experimenter is applying forces to move the joint. In position control, unstable and non-repetitive fluctuations appear. A sample of the results from both model 1 and 2 are shown on Fig.2 while a constant active motor torque of 13 Nm is applied and motion is physically controlled by the experimenter.

The three elements, i.e. the motor inertia, the robot structure under the gravitational force and the active/dissipative change of efficiency, have an important contribution to the torque applied at the robotic joint. The torque models are evaluated in functions of the root-mean-square deviation RMSD over the nominal torque range of the motor (about 44 Nm). Torque model 1 reports an RMSD of 6.6 to 7.6 Nm while model 2 has an RMSD of 4.3 to 4.8 Nm. Model 2 presents more precise torque estimations as the motor torque augment.

D. *Discussion*

The identified hip joint's impedance of the exoskeleton, as defined by model 2, presents an RMSD about 4.5 Nm. In comparison with the continuous torque capacity of the motor reported at the joint, between 24 Nm and 57 Nm, the deviation seems quite high (8-19% of the continuous torque). However, the deviation recorded seems to be mostly due to noise in the acquisition of the acceleration, see Fig.2, and the following estimation of the effect of inertia. Oscillations at high frequencies are nevertheless damped through the electric inductance of the motor, the impedance of the transmission units and eventually the physical interface with the user. On average, the error between the identified model and the measured torque varies between 0.5 and 3.5 Nm. Regarding the latter result, an open loop control with an estimation of the torque transmitted to the user based on model 2 is judged satisfying as the error lies within 10% of the desired torques.

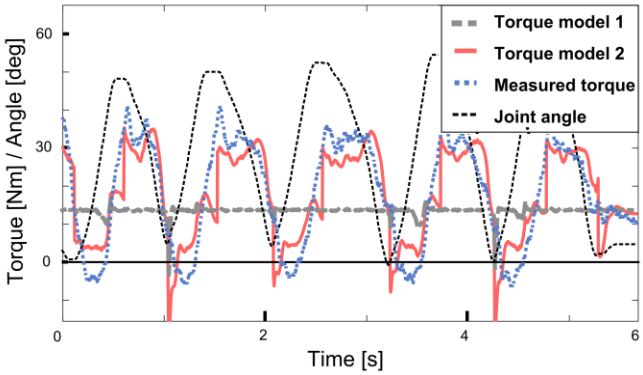

Figure 2. Illustration of estimated model 1 (active torque) and model 2 for the torque at the robotic hip joint in comparison with the measured torque. The angle is given here to show the motion of the joint. A constant motor torque is applied while the experimenter is moving the robotic joint.

III. Three-Phases Variable Impedance Gait Assistive Strategy

The human biological actuation units are composed of muscles and tendons, which are fastened to bones distant one from the other by one or more joints. Such actuation units can be seen as series elastic actuators because of the compliance of both muscle and tendon tissues. The conjunction of agonist and antagonist muscles turns the body joints into variable impedance systems. Human locomotion strategies are largely built on these characteristics to ensure both stability and energetically optimized performance. Variable stiffness controllers mimic biological strategies to better assist the pilot while being user friendly.

The key characteristics of a good assistance are the following: first, it should transfer a notable amount of force to the user in order to augment her/his performances or in order to compensate for a lack of strength. Second, it should minimally constrain the user temporally or spatially. An exception is the presence of compensatory or pathological motions that need to be constrained to avoid clinical complications by the user (e.g. knee hyperextension during stance).

A. *Variable impedance controller*

The hypothesis underlying this approach comes from the fact that joint impedance during activities such as walking appears to mimic a spring effect with variable stiffness over a limited number of phases. Gait dynamics and kinematics from D. Winter [22] and S. Ounpuu [23] can be represented graphically to highlight this spring-like behavior as shown on Fig.3 for the hip flexion/extension.

It is hypothesized that the natural gait is generated with constant joint stiffness during two intervals similar to the stance and swing phases lasting both about 40% of the cycle. The two double support phases, each about 10% of the cycle are reported as transitional states.

The muscle contribution is modeled as a spring effect about the joint. We propose to transmit a similar impedance effect through the wearable exoskeleton. Equation (8)

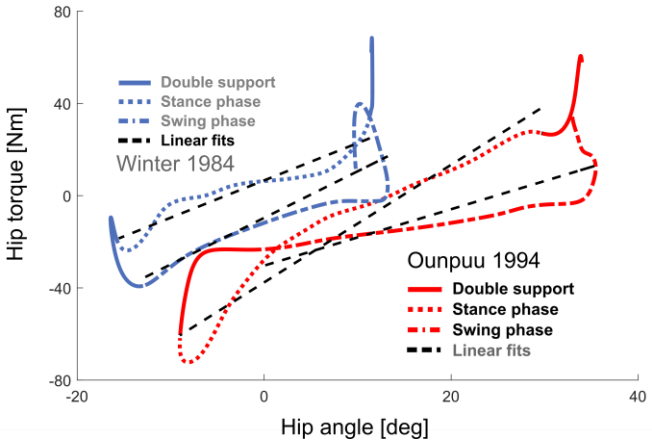

Figure 3. Hip flexion/extension torque during walking versus hip angle as reported in the literature by Winter and Ounpuu [22], [23]. Curves are split along the different gait phases, i.e. double support, stance and swing phases, to highlight the constant spring-like phase-related behavior.

expresses the natural torque at the joint where k_m is the muscle-tendon stiffness and α_0 is the angle at equilibrium. Equation (9) is the torque resulting from the addition of an impedance controller through the exoskeleton to the muscle activity, where k_{exo} and α_{0exo} are the simulated stiffness and angle at equilibrium by the exoskeleton. The final impedance of the joint assisted by the exoskeleton is reported in (10) for the stiffness and (11) for the angle at equilibrium.

$$\tau_{joint} = k_m \cdot (\alpha - \alpha_0) \quad (8)$$

$$\tau_{joint}{}' = k_m' \cdot (\alpha - \alpha_{0m}') + k_{exo} \cdot (\alpha - \alpha_{0exo}) \quad (9)$$

$$k_{assisted} = k_m' + k_{exo} \quad (10)$$

$$\alpha_{0assisted} = \frac{k_m' \cdot \alpha_{0m}{}' + k_{exo} \cdot \alpha_{0exo}}{k_m' + k_{exo}} \quad (11)$$

Equations (8) to (10) show that the contribution of the muscles and the exoskeleton are linearly and proportionally combined. Simultaneously, the resulting angle at equilibrium is the weighted average between the individual angles at equilibrium over the individual stiffness ratios. Thus, the range of motion and level of assistance can easily be modulated following the controller's angle and stiffness parameters.

B. *Phase detection*

As discussed above, the controller consists of the simulation of impedance behaviors that evolves over the different phases of gait. A robust way to detect stance and swing phases is to use contact or force sensors under the feet. However, an approach based on the kinematics is proposed and is able to predict motion intentions while the foot is still in contact or before it is in contact with the ground. Nevertheless, it is weaker in terms of robustness.

Initial investigations indicate that the hip flexion velocity is a good predictor for the detection of the different impedance states. Three phases are proposed as candidates and are called "hip flexing", "hip extending" and "static" phases. These phases are similar, respectively, to the swing, stance and double support standard phases. Equations (12)-(14) express the conditions for such phase detection, where V_{hip} is the velocity measured at the hip joint on the reference side (e.g. left hip), V_{opp_hip} is the velocity measured at the opposite side (e.g. right hip), V_{lim+} is a constant parameter defining the phases' limits.

Similarly, during the swing and (single) stance phases, the hip flexing and hip extending phases are intended to be mirrored in both the left and right legs. In order to ensure the symmetry of the controller, the same event is tested on both legs (12) and (13) to detect flexion. In case of a hip flexing phase on one leg, the opposite leg is automatically turned into hip extending mode. When neither leg is flexing, either the user is not walking or she/he is walking and in a transition state. The different phases and impedance of the controller in the context of gait initiation, continuous walking and gait termination are illustrated on Fig.4.

Hip flexing phase condition: $V_{hip} > V_{lim+}$ (12)

Hip extending phase condition: $V_{opp\_hip} > V_{lim+}$ (13)

Static phase conditions: $V_{hip} \leq V_{lim+}$ and $V_{opp\_hip} \leq V_{lim+}$ (14)

C. *Management of gait initiation and termination*

The phase detection allows coordination of the controller by the motion of the user. A weak phase detection would lead to poor assistive results. Gait initiation and termination with poor detection performances could lead to hazardous stepping or immobilization of the user with potential dramatic consequences. As the controller targets individuals with significant muscle weakness, particular attention is aimed at the metrics of gait initiation and termination. The metrics of the study are selected to be the delay between the intention of motion and the effective detection of this intention and the amount of force the user need to apply before the system detects an intention. As presented on Fig.3, the detection of gait initiation or termination uses the same scheme as for the phase detection.

1) *Gait initiation*

To initiate gait, the user stands in the still position which corresponds to the static phase of the controller. In order to start walking, flexion of one hip up to the velocity threshold V_{lim+} should be induced such that the controller phase will turn into hip flexing for one leg and hip extending for the

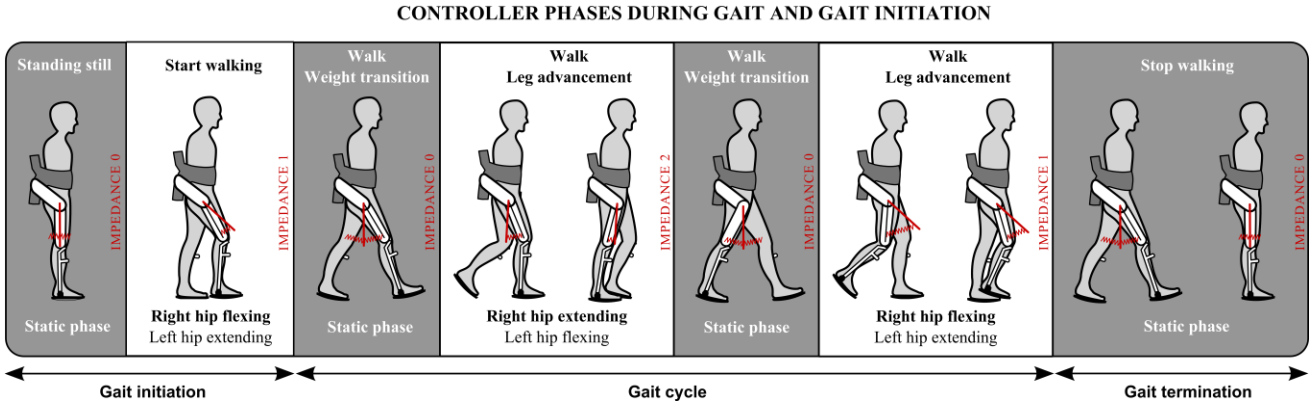

Figure 4. Illustration of the different phases of the controller from gait initiation to termination through a full gait cycle. Impedance is represented by its theoretical mechanical equivalent which is a fixed element linked to the femur segment by spring. The fixed element (i.e. large bar) reflects the simulated equilibrium angle.

opposite leg. The user must provide enough force to trigger a flexion motion. This force depends on both the passive and active impedance, which are mainly the dry friction and the torque in static phase. The force is also function of parameters, i.e. the velocity threshold V_{lim+}.

Time delay and triggering torques required to pass from a static to a hip flexing phase are investigated using the same setup as for the characterization of the actuation unit where the force is operated by hand through a force sensor. The experiment comports six values of V_{lim+} ranging from 10 to 100 [deg/s] and four values of stiffness in static phase from 0.5 to 3.0 [Nm/deg]. Results are presented on Fig.5 for the detection delay and torque required. Each data are averaged over a repetition of five measurements.

2) Gait termination

Gait termination is defined as the controller turns into static phase and stays in that phase. The transition from flexing/extending phases to static phase is usually natural. It can occur either as the swinging leg reaches a stable (maximum) angle of flexion or as the wearer makes early contact with the ground. The static phase occurs at the end of each flexing phases, as the hip direction needs to revert to go forward. Gait can thus be terminated at the end of any step.

3) Influence of parameters

Results of investigations on gait termination are provided on Fig.5. Globally, one can denote that the parameters of velocity and stiffness have opposite effects on the detection of initiation versus termination. The delay and torque necessary for initiating walking increase with the velocity threshold and the controller stiffness in static phase. Thus, a low velocity threshold is more adapted for people with muscle weakness. However, time delay and torque required to stop walking are lowered by increasing the velocity threshold and the static phase's stiffness parameter. In fact, when the velocity threshold is low, the controller can misinterpret tiny motions with intentions of motion and can induces unwanted oscillations. A good compromise between stability and low initiation torque can be found in a range of velocity threshold between 30 and 60 [deg/s].

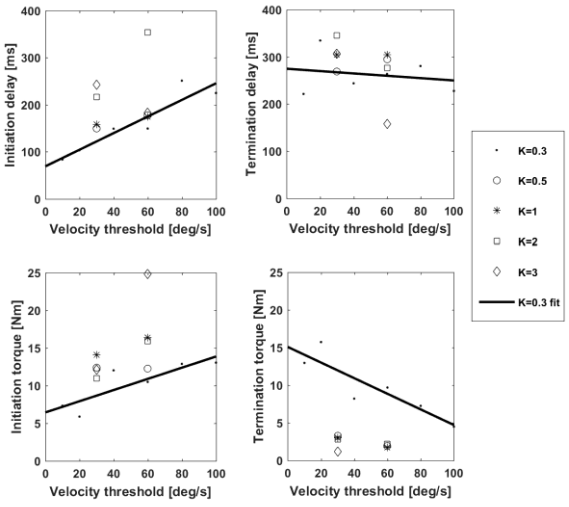

Figure 5. Effects of the velocity threshold V_{lim+} and stiffness parameter K in the static phase, (top) on the delays and (bottom) on the triggering torques.

IV. Evaluation of the Control Strategy

The three-phase variable impedance gait assistive strategy is used in a haptic context where the human-robot interaction is bi-directional. It is important for the evaluation to take place in the context defined originally, i.e. in overground walking with the exoskeleton in assistance mode.

A. Method

Two pilots, one healthy and one with a neuromuscular disease (NMD) walked about 12 meters with the AUTONOMYO exoskeleton. Both pilots were similar in height and weight (about 185cm and 70-80kg). The affected pilot has a limb girdle muscular dystrophy with quasi-symmetrical strength in the lower limbs which is: good about ankle dorsi- and plantar flexion, moderate about hip and knee extensions and poor about hip and knee flexions.

The exoskeleton is controlled with the three-phase variable impedance strategy, where the impedance mimics a spring mechanism. A damping effect is also provided during the flexing and extending phases in order to avoid instability in the controller and particularly during transition between phases. The general form of the impedance is written in (15), while the parameters depending on the phase and on the pilots are reported in Table I.

$$\tau_{assist} = k \cdot (\alpha - \alpha_0) - \lambda \cdot \dot{\alpha} \quad (15)$$

Where τ_{assist} is the torque provided to the pilot by the exoskeleton, k is the simulated spring stiffness, α_0 the simulated equilibrium angle and λ is the viscosity coefficient. The impedance parameters have been tuned in accordance with the pilots' feedback and in adequacy with the walking velocity. The evaluation of the controller is made considering its coherence with regards to the torque profiles from the literature. At this stage, the impact of the assistance on the energy expenditure or muscle activity has not been investigated.

TABLE I. Parameters of Impedance at the Hip for the Different Phases and Pilots

	Impedance parameters			
	Healthy pilot		**Pilot with NMD**	
Phases	***k* [Nm/deg]**	**α_0 [deg]**	***k* [Nm/deg]**	**α_0 [deg]**
Static phase	0,8	0	0,2	5
Flexing phase	1,5	30	0,6	30
Extending phase	1,4	0	0,4	-5
	Viscosity coefficient λ = 0.11 [Nm s/deg]			

B. Results

Both pilots were able to initiate and terminate walking at their convenience. The velocity threshold for the pilot with NMD is set to 20 deg/s while for the healthy pilot the value of 50 deg/s is good. The pilot with NMD requires a physical support in order to keep his balance while walking with the exoskeleton (can walk without the exoskeleton using a cane).

Fig.6 illustrates the hip angles and torques over one gait cycle (average over N>10 walking steps). The angles and torques from the literature are also reported in Fig.6. However walking kinematics and dynamics from the

literature corresponds to higher walking velocity than gait performed by pilots wearing the exoskeleton.

1) Hip flexion/extension trajectories

Ranges of motion (RoM) at the hip are respectively of 47deg and of 31deg for the healthy and the NMD pilots. The NMD pilot reaches the full extension early at 35% of the gait cycle while the healthy pilot reaches it about 47%. Both are in advance regarding the literature where the maximal extension is reached about 50-55% of the gait cycle. The assisted gait present both an overshoot of flexion about 6deg preceding heel strike. The healthy pilot has a short flexing phase with a high flexing velocity compared to a long flexing phase with low velocity for the NMD pilot. However, the static phase following the flexion is especially long for the healthy pilot.

2) Hip flexion/extension torque

The assistance torques for the healthy and the NMD pilots are very similar during the extending phase, the following static phase and the beginning of the flexing phase. These torque patterns from 10% to 85% of the gait cycle are similar but smaller than the torques from the literature. About the event of heel strike, however, high extension torques are reported in the literature, whereas the controller provides very small torques during this static phase. This aspect is discussed in the following.

C. Discussion

Both the healthy and the NMD pilots reported a synchronous and non-constraining motion of the exoskeleton while walking. In both cases, the action of the exoskeleton was reported as positive and impactful. Some differences in kinematics and torque patterns from the use of the exoskeleton compared to natural gait from the literature can be observed. The most notable event is the long static phase experienced by the healthy user wearing the exoskeleton during the heel strike event. During natural walking, one tends to have a continuous forward motion of the center of mass (CoM) in order to lower the energy cost. In the case of wearing the exoskeleton, the transition phase (static phase during heel strike) is managed differently compared to non-assisted gait. First, the exoskeleton does not provide a push-off phase that comes originally from a strong flexion propulsion of the ankle. Secondly, it is carefully designed to ensure that the motion is quickly stopped during double support so that the pilot has the possibility to terminate gait without much effort.

The assistive torques provided reach about 70% of peak torques reported by Stoquart et al. on treadmill for a bodyweight of 70 kg [24] at a walking velocity of 2 km/h. Further comparisons have not been made since the dynamics are quite different between treadmill and overground walking.

V. Conclusion

Rigid transmissions offer the possibility to simulate impedance control where the level of accuracy lies within the dry friction range of torques. Active impedance allows a wide range of possibilities and evolutions that would be limited while using mechanical solutions such as series elastic actuators; although, active impedance is less energetically efficient as it can poorly store energy.

Using a rigid transmission over the hip joint of the AUTONOMYO exoskeleton, a full gait assistive strategy based on finite-state control is presented. Designed for people with muscle weakness or neurological disorders, particular attention is paid towards the triggers for the walking initiation and termination. A method actively involving the pilot in the gait through a detection of intention based on the hip flexion is presented. Results (Fig.5) show that torques under 8Nm in flexion of the hip over a duration of 150ms are sufficient to control the device. The control strategy based on three states that are quite similar to the stance, swing and double support phases of the gait allows to provide a powerful assistive controller free from spatial and temporal constraints. Moreover, impedance offers an easy and intuitive tuning of assistance level and stride length.

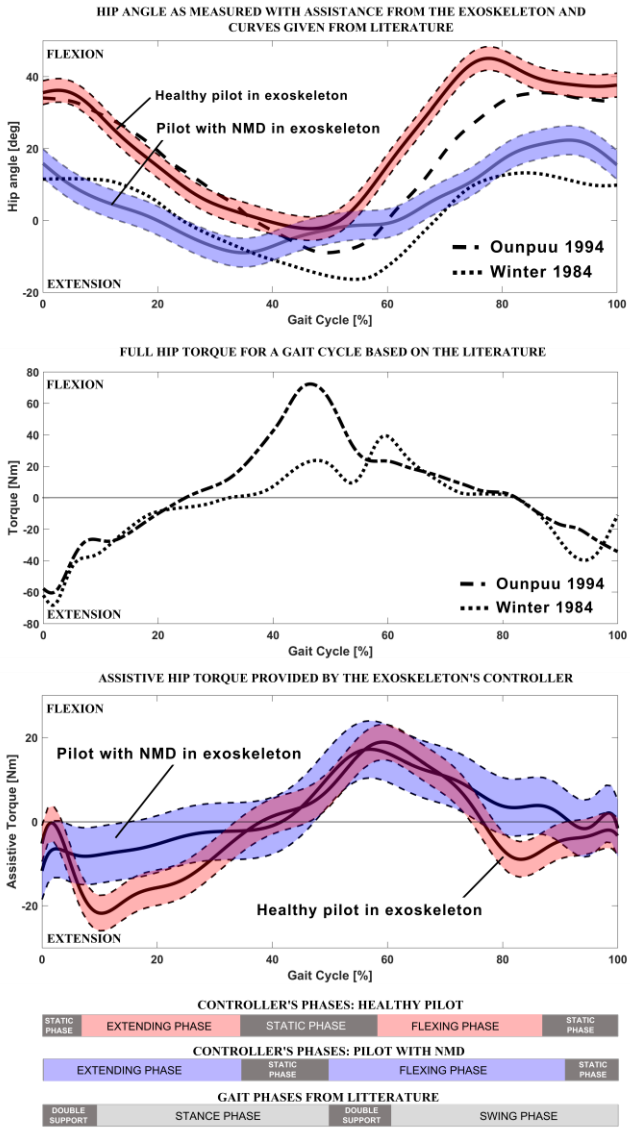

Figure 6. Kinematic and dynamic results of a healthy pilot and a pilot with a neuromuscular disease (NMD) assisted by the exoskeleton, and data from the literature with healthy adults.

A preliminary evaluation of the controller has been performed with a healthy pilot and a pilot with neuromuscular disease. Experimentations confirmed the similarities between the resulting controlled torques and the natural torques during gait from the literature. Meanwhile some differences persist, they are inherent of mechanical aspects such as the constrained range of motion at the ankle or the viscosity in the robotic joints at high velocities.

Future work will investigate the effect of such active variable impedance controller on different populations affected by muscular weakness and neurological disorders.

REFERENCES

[1] R. Riener, L. Lunenburger, S. Jezernik, M. Anderschitz, G. Colombo, and V. Dietz, "Patient-cooperative strategies for robot-aided treadmill training: first experimental results," *IEEE Transactions on Neural Systems and Rehabilitation Engineering*, vol. 13, no. 3, pp. 380–394, Sep. 2005.

[2] J. F. Veneman, R. Kruidhof, E. E. G. Hekman, R. Ekkelenkamp, E. H. F. V. Asseldonk, and H. van der Kooij, "Design and Evaluation of the LOPES Exoskeleton Robot for Interactive Gait Rehabilitation," *IEEE Transactions on Neural Systems and Rehabilitation Engineering*, vol. 15, no. 3, pp. 379–386, Sep. 2007.

[3] L. Marchal-Crespo and D. J. Reinkensmeyer, "Review of control strategies for robotic movement training after neurologic injury," *Journal of NeuroEngineering and Rehabilitation*, vol. 6, p. 20, Jun. 2009.

[4] S. K. Au, J. Weber, and H. Herr, "Powered Ankle–Foot Prosthesis Improves Walking Metabolic Economy," *IEEE Transactions on Robotics*, vol. 25, no. 1, pp. 51–66, Feb. 2009.

[5] S. Au, M. Berniker, and H. Herr, "Powered ankle-foot prosthesis to assist level-ground and stair-descent gaits," *Neural Networks*, vol. 21, no. 4, pp. 654–666, May 2008.

[6] K. Fite, J. Mitchell, F. Sup, and M. Goldfarb, "Design and Control of an Electrically Powered Knee Prosthesis," in *2007 IEEE 10th International Conference on Rehabilitation Robotics*, 2007, pp. 902–905.

[7] B. E. Lawson, A. H. Shultz, and M. Goldfarb, "Evaluation of a coordinated control system for a pair of powered transfemoral prostheses," in *2013 IEEE International Conference on Robotics and Automation*, 2013, pp. 3888–3893.

[8] M. Liu, F. Zhang, P. Datseris, and H. (Helen) Huang, "Improving Finite State Impedance Control of Active-Transfemoral Prosthesis Using Dempster-Shafer Based State Transition Rules," *J Intell Robot Syst*, vol. 76, no. 3–4, pp. 461–474, Dec. 2014.

[9] D. Zlatnik, B. Steiner, and G. Schweitzer, "Finite-state control of a trans-femoral (TF) prosthesis," *IEEE Transactions on Control Systems Technology*, vol. 10, no. 3, pp. 408–420, May 2002.

[10] C. D. Hoover, G. D. Fulk, and K. B. Fite, "Stair Ascent With a Powered Transfemoral Prosthesis Under Direct Myoelectric Control," *IEEE/ASME Transactions on Mechatronics*, vol. 18, no. 3, pp. 1191–1200, Jun. 2013.

[11] D. L. Grimes, "An active multi-mode above knee prosthesis controller," Thesis, Massachusetts Institute of Technology, 1979.

[12] A. W. Boehler, K. W. Hollander, T. G. Sugar, and D. Shin, "Design, implementation and test results of a robust control method for a powered ankle foot orthosis (AFO)," in *2008 IEEE International Conference on Robotics and Automation*, 2008, pp. 2025–2030.

[13] Y. D. Li and E. T. Hsiao-Wecksler, "Gait mode recognition and control for a portable-powered ankle-foot orthosis," in *2013 IEEE 13th International Conference on Rehabilitation Robotics (ICORR)*, 2013, pp. 1–8.

[14] R. J. Farris, H. A. Quintero, and M. Goldfarb, "Performance Evaluation of a Lower Limb Exoskeleton for Stair Ascent and Descent with Paraplegia," *Conf Proc IEEE Eng Med Biol Soc*, vol. 2012, pp. 1908–1911, 2012.

[15] S. Murray and M. Goldfarb, "Towards the use of a lower limb exoskeleton for locomotion assistance in individuals with neuromuscular locomotor deficits," in *2012 Annual International Conference of the IEEE Engineering in Medicine and Biology Society*, 2012, pp. 1912–1915.

[16] H. A. Quintero, R. J. Farris, C. Hartigan, I. Clesson, and M. Goldfarb, "A Powered Lower Limb Orthosis for Providing Legged Mobility in Paraplegic Individuals," *Top Spinal Cord Inj Rehabil*, vol. 17, no. 1, pp. 25–33, 2011.

[17] H. Kawamoto, S. Kanbe, and Y. Sankai, "Power assist method for HAL-3 estimating operator's intention based on motion information," in *The 12th IEEE International Workshop on Robot and Human Interactive Communication, 2003. Proceedings. ROMAN 2003.*, 2003, pp. 67–72.

[18] Y. Sankai, "HAL: Hybrid Assistive Limb Based on Cybernics," in *Robotics Research*, Springer, Berlin, Heidelberg, 2010, pp. 25–34.

[19] A. Ortlieb, M. Bouri, R. Baud, and H. Bleuler, "An assistive lower limb exoskeleton for people with neurological gait disorders," in *2017 International Conference on Rehabilitation Robotics (ICORR)*, 2017, pp. 441–446.

[20] A. Ortlieb, J. Olivier, M. Bouri, H. Bleuler, and T. Kuntzer, "From gait measurements to design of assistive orthoses for people with neuromuscular diseases," in *2015 IEEE International Conference on Rehabilitation Robotics (ICORR)*, 2015, pp. 368–373.

[21] R. Baud, A. Ortlieb, J. Olivier, M. Bouri, and H. Bleuler, "HiBSO Hip Exoskeleton: Toward a Wearable and Autonomous Design," in *New Trends in Medical and Service Robots*, 2016, pp. 185–195.

[22] D. A. Winter, "Kinematic and kinetic patterns in human gait: Variability and compensating effects," *Human Movement Science*, vol. 3, no. 1–2, pp. 51–76, Mar. 1984.

[23] S. Ounpuu, "The biomechanics of walking and running," *Clin Sports Med*, vol. 13, no. 4, pp. 843–863, Oct. 1994.

[24] G. Stoquart, C. Detrembleur, and T. Lejeune, "Effect of speed on kinematic, kinetic, electromyographic and energetic reference values during treadmill walking," *Neurophysiologie Clinique/Clinical Neurophysiology*, vol. 38, no. 2, pp. 105–116, Apr. 2008.